Research Article

Structural Health Monitoring Using Wireless Technologies: An Ambient Vibration Test on the Adolphe Bridge, Luxembourg City

Adrien Oth[1] and Matteo Picozzi[2]

[1] *European Center for Geodynamics and Seismology (ECGS), 19 Rue Josy Welter, 7256 Walferdange,*
   Grand Duchy of Luxembourg, Luxembourg
[2] *Helmholtz Centre Potsdam-GFZ German Research Centre for Geosciences, Telegrafenberg, 14473 Potsdam, Germany*

Correspondence should be addressed to Adrien Oth, adrien.oth@ecgs.lu

Major threats to bridges primarily consist of the aging of the structural elements, earthquake-induced shaking and standing waves generated by windstorms. The necessity of information on the state of health of structures in real-time, allowing for timely warnings in the case of damaging events, requires structural health monitoring (SHM) systems that allow the risks of these threats to be mitigated. Here we present the results of a short-duration experiment carried out with low-cost wireless instruments for monitoring the vibration characteristics and dynamic properties of a strategic civil infrastructure, the Adolphe Bridge in Luxembourg City. The Adolphe Bridge is a masonry arch construction dating from 1903 and will undergo major renovation works in the upcoming years. Our experiment shows that a network of these wireless sensing units is well suited to monitor the vibration characteristics of such a historical arch bridge and hence represents a low-cost and efficient solution for SHM.

1. Introduction

In order to ensure the structural stability of strategic civil infrastructure such as bridges, large dams, or high-rise buildings, the systematic monitoring of these (preferably on a continuous basis) is an issue of prime importance. This statement is, of course, particularly true in earthquake-prone regions. Picozzi et al. [1], for instance, show how a seismic monitoring system of low-cost wireless sensors can be employed for the surveillance of the behavior of buildings damaged by strong ground shaking from a major earthquake (in their case, the 2009 Mw 6.3 Aquila event) during the earthquake's aftershock sequence, which can provide invaluable information in order to ensure the safety of rescue teams during postevent relief operations.

Nevertheless, in areas less exposed to seismic hazard, such monitoring techniques also represent important tools for civil engineers, for instance, if they have to deal with structures exposed to heavy operational demands for extended periods of time and whose structural integrity might be in question or at risk. A continuous monitoring of such structures allows for an identification of their fundamental response characteristics and the changes of these over time, the latter representing indicators for potential structural degradation.

A good example for such a case is the Adolphe Bridge in Luxembourg City. Linking the two city quarters on opposite sides of the Vallée de la Pétrusse, the Adolphe Bridge was designed as an open spandrel arch and officially opened in 1903. Since the bridge is connecting the Upper City of Luxembourg with the railway station, it is subjected to heavy traffic (in particular buses), which has considerably weakened the structure over the years since the first renovations that were performed in 1961/62. Moreover, with the LuxTram project (http://www.luxTram.lu/) destined to reintroduce tramway traffic to Luxembourg, major renovation of the bridge is necessary and expected to be launched in 2011. Following these renovations, the real-time monitoring of the bridge's vibrations could help in assessing the success of these efforts, as well as the bridge's performance on a continuous basis in the future.

In recent years, techniques based on ambient vibration recordings have become a popular tool for characterizing the seismic response and state-of-health of strategic civil infrastructure (e.g., [2–4]). The primary advantage of these approaches lies in the fact that no transient earthquake signals or even active excitation of the structure under investigation are required. Ditommaso et al. [5] investigated the response characteristics of the Falkenhof Tower in Potsdam, Germany, using interferometric and time-frequency analysis techniques, using both ambient noise and records obtained from a near-by explosion. Prieto et al. [6] performed a similar study using ambient noise records obtained in a 17-storey instrumented building at the University of California in Los Angeles, and Picozzi et al. [7] tested the suitability of a system of low-cost wireless sensing units for real-time monitoring of large-scale infrastructure using the example of the Fatih Sultan Mehmet Suspension Bridge in Istanbul.

As a first step towards proposing a continuous monitoring approach for the Adolphe Bridge and in order to validate the performance of this novel wireless system for structural monitoring on such a historical arch bridge (representing a critical infrastructure for the city of Luxembourg), we carried out ambient vibration measurements on 11 May 2010, using a very dense network composed of 18 wireless sensing units deployed at regular intervals along the bridge deck. We recorded several hours of ambient vibrations generated primarily by human activity, that is, by the traffic crossing the bridge. Using these recordings, we analyze the response characteristics of the Adolphe Bridge and empirically determine the resonance frequencies and modal shapes of the structure as well as attempt to derive the damping characteristics.

2. The Adolphe Bridge: A Brief Overview

With the dismantlement of the fortress of Luxembourg starting in 1867, the city continually expanded on the Plateau Bourbon located on the opposite side of the Vallée de la Pétrusse, which encircles the Upper City (i.e., the city center and core of the old fortress) of Luxembourg. At the end of the 19th century, the only connection between these new quarters and the Upper City was a rather narrow viaduct dating back to the fortress time. Since the railway station of Luxembourg had already been built on the Plateau Bourbon, there was an urgent need to ensure its proper connection to the Upper City by an additional link to account for these rapid developments. Therefore, between 1900 and 1903, during the reign of Grand Duke Adolphe, the Adolphe Bridge was constructed to accommodate this situation and the therewith increased traffic needs. A detailed discussion on the history of the Adolphe Bridge and the adopted construction principles can be found in Wirion and Heinerscheid [8].

The Adolphe Bridge (Figure 1), officially opened on 24 July 1903, is a masonry arch construction (2 identical arch constructions on the left and right, Figure 1(b)) with a length and width of 153 m and 17.2 m, respectively. The span of the central arches amounts to 84.65 m, while the smaller arches on both sides of the central ones have a span of 21.6 m each.

Significant rehabilitation works were carried out during the years 1961/62, where the original bridge deck was integrally replaced and the new deck was at the same time enlarged by 0.5 m on both sides.

During the 1990s and early 21st century, it was noted that the bridge showed notable structural deficiencies, in particular related to cracks in the arch masonries [9]. Therefore, in order to ensure its structural stability, provisional safety measures were undertaken and prestressed steel bars introduced in the central arches during the years 2003/2004. In order to permanently remedy the situation and in view of the LuxTram project, the aim of which lies in the reintroduction of tramway traffic in Luxembourg that would also cross the Adolphe Bridge, major rehabilitation works will take place starting in 2011, with an expected duration of approximately four years. These renovation works are undertaken by order of the Luxembourgish Government, represented by the Minister for Sustainable Development and Infrastructures, for which the Director of the *Administration des Ponts et Chaussées* manages the project. These works are also supervised by the *Administration des Ponts et Chaussées*, and amongst other measures, the bridge deck will be renewed and the arches stabilized with reinforced concrete.

The vibration characteristics of the bridge in its original state were investigated in a forced vibration experiment performed in October 1933 [10], in which the author came to the conclusion that the fundamental frequency of resonance of the bridge was around 4 Hz.

3. Ambient Vibration Measurements and Data Processing

On 11 May 2010, we performed ambient vibration measurements on the Adolphe Bridge using a set of 18 low-cost wireless sensing units (WSUs) (Figure 1(c)) developed by the GFZ German Research Centre for Geosciences in Potsdam and the Department of Informatics of Humboldt University Berlin within the framework of the EU FP6 project "Seismic eArly warning For EuRope" (SAFER) and the "Earthquake Disaster Information system for the Marmara region, Turkey" (EDIM) project, originally intended for earthquake early warning purposes. Yet as shown by Picozzi et al. [7, 11], these WSUs are also highly attractive for monitoring critical infrastructure.

Each WSU (Figure 1(d)) is composed of a low-cost three-component seismic sensor (thus far either a build-in accelerometer or an external 4.5 Hz geophone), a digitizer board with an effective resolution of 19 bit, onboard storage capability provided by a CompactFlash card and, as the designation "wireless sensing unit" indicates, wireless data transmission capabilities. In particular, the last point is of great importance, since this capability can be used to assemble a large number of WSUs to a self-organizing network and send the recorded data via wireless connections to a central data acquisition center. In such a self-organizing network, each unit is in direct contact with its neighboring units and serves as a sender and receiver of information. This principle enables a unit that is not in direct contact

Luxembourg-11/05/2010

18 sosewin + 4.5 Hz geophones
Recording time: 9:00 UTC–17:00 UTC

(a)

(b)

Official name: Pont Adolphe
Design: Open spandrel Arch
Total length: 153 m
Width: 17.2 m
Longest span: 84.65 m
Clearance below: 42 m
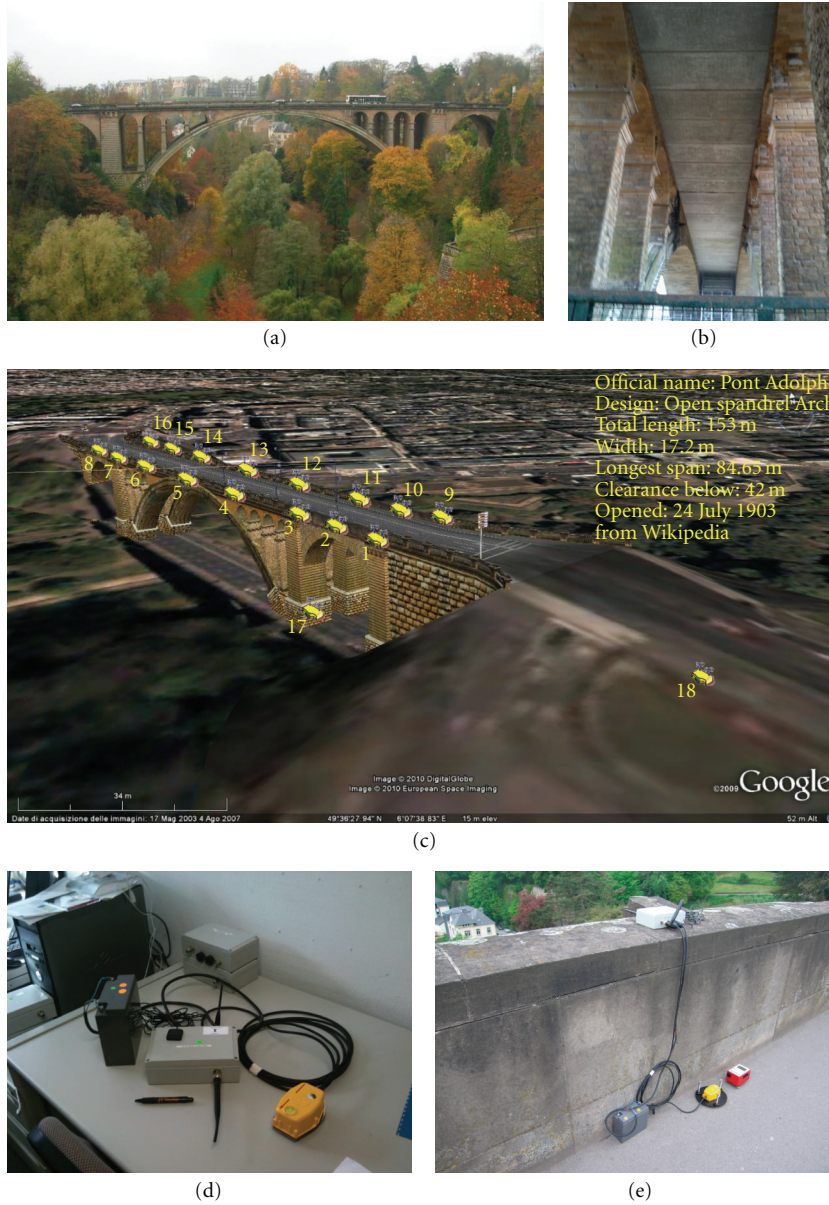Opened: 24 July 1903
from Wikipedia

(c)

(d)

(e)

FIGURE 1: Photos of the Adolphe Bridge and instruments used and information on the measurement setup. (a) Sideview of the Adolphe bridge (source: Wikimedia Commons). (b) View from below. (c) Measurement setup used on the Adolphe bridge. (d) Wireless sensing unit (WSU) used for the ambient vibration measurements on the Adolphe bridge. The central part of the unit, including the digitizing board, is contained in the box shown in the center of the picture, with antennas for wireless data transmission. The 4.5 Hz geophone is the yellow instrument shown on the right. On the left, the battery providing the necessary power supply is depicted. (e) Deployment of one WSU on the bridge walkways. The geophone (yellow) is centered in a horizontal position on the walkway, with the two horizontal components oriented in the longitudinal and transverse direction with respect to the bridge, respectively. The red object in the picture is a Tromino® sensor deployed by the Geological Survey of Luxembourg for comparative purposes.

with the central acquisition unit to still pass its information to the latter via several transmitting WSUs. Moreover, in the case of failure of one or several units, the network has the ability to reorganize itself such that the information of all working WSUs always reaches the acquisition point.

If the transmission of the entire recorded data is not desired/required, each WSU can also perform a predefined set of calculations on the recorded data and only transmit the calculated parameters to the central acquisition center. For an in-depth discussion of the technical characteristics of the

WSUs, we refer the reader to Fleming et al. [12] and Picozzi et al. [7, 11].

For our measurements on the Adolphe Bridge, we used a total of 18 WSUs equipped with 4.5 Hz three-component geophones as sensors, and we recorded the ambient vibrations with a sampling rate of 100 samples/sec. Therefore, we are able to examine a wide frequency range (i.e., 1–25 Hz) that includes the modal frequencies of resonance of the bridge.

The setup of the experiment is shown in Figure 1(c). Since this work was intended as a feasibility study and the access into the arch structure is subject to strict safety regulations requiring nonnegligible costs and organizational efforts, we chose a measurement setup that was easiest to implement and still enabled us to obtain good information on the bridge's vibration characteristics. We positioned 8 WSUs on the walkways along each side of the bridge (sensors 1–8 on the left, looking from the railway station towards the Upper City, and sensors 9–16 on the right side). In the case of a permanent installation for the purpose of continuous monitoring of the bridge, sensors should of course be also installed within the arch structure of the bridge.

We furthermore installed two additional sensors, the first of which was fixed at the bottom of one of the bridge's pillars (sensor 17) and the second one approximately 50 m away from the bridge close to the Banque et Caisse d'Epargne de l'Etat (BCEE) building at the Place de Metz square (sensor 18) (see also Figure 1(c)). The main idea behind installing sensor 17 was to perform an interferometric analysis in order to derive seismic wave propagation velocities within the pillar. However, the coupling of the sensor to the pillar was, unfortunately, not optimal, preventing us from obtaining clear results. Sensor 18 on the other hand was intended as a reference outside the bridge. Since this sensor, however, still showed a relatively strong influence of the bridge's vibrations and the resonance characteristics were well recognizable directly from the Fourier power spectra at each sensor without the necessity to calculate spectral ratios relative to an outside reference (as we show below), we do not make further use of the recordings obtained at sensor 18.

Figure 1(e) shows the deployment of a WSU on the bridge deck. The geophone was oriented such that the two orthogonal horizontal components pointed in the longitudinal and transverse direction relative to the bridge. Each WSU transmitted the recorded data directly to a laptop installed close to sensor 1. We recorded approximately from 09:00 to 17:00 UTC, and in the following, we show the bridge characteristics derived using 5 hours of data, from 10:00 to 15:00 UTC. As an example of the recorded ambient vibrations, Figure 2 shows a 50 min extract of the records on the vertical component at eight sensors along the bridge (4 on each side, i.e., sensors 2, 4, 5, 7 on the left and sensors 10, 12, 13, 15 on the right side). As expected, the records show a large number of transient signals, which are related to the traffic on the bridge. The signals at the different sensors show clear variations in their amplitudes, depending on sensor's position, thus reflecting the different strengths vibration at different points along the bridge. While the amplitudes are largest at sensor pairs (4, 12) and (6, 14), approaching the center of the bridge, the vibrations induced by the traffic diminish when approaching the edges.

4. Spectral Characteristics of the Adolphe Bridge

For each sensor and each of the three components of motion, we determined the power spectral density (PSD) for the measurement duration of 5 hours mentioned previously following McNamara and Buland [13]. For this purpose, the data are split into a series of short time windows of one-minute length each, and for each of these windows, the Fourier power spectral density (PSD) is calculated. Then the average and standard deviation over all time windows are determined and this averaged PSD is expressed in decibel (dB). If the structure under consideration shows strong resonance effects, we expect to see clearly identifiable peaks immediately in these average PSD estimates without any additional processing.

The obtained average PSD estimates for the same eight sensors shown in Figure 2 are depicted in Figures 3 (vertical component), 4 (transversal component), and 5 (longitudinal component). A first observation is that, in general, the power spectral densities are well constrained, with overall small standard deviations (the largest standard deviations are mostly located at the lowest frequencies of analysis between 1 and 2 Hz). This shows that the spectra are very stable over the investigated 5-hour time window, a fact that is also confirmed by examining more closely the spectrograms (one example is shown in Figure 6(a)). One might expect to see some differences in PSD estimates obtained during day and night, since the traffic load of the bridge is obviously subject to strong temporal fluctuations. In order to clarify this issue, we performed a set of comparative measurements for a total of 45 min duration at the locations of sensors 2 and 5 (Figure 1) on a late Sunday evening (30 January 2011) using a Tromino® sensor provided by the *Service Géologique del'Administration des Ponts et Chaussées*. However, no significant differences in the PSD estimates could be detected when compared with the daytime measurements of 11 May 2010.

The PSD estimates shown in Figures 3, 4, and 5 show distinct peaks corresponding to the resonance frequencies of the bridge. Since these peaks are very clear, it is not necessary to perform spectral ratio calculations relative to a reference station uninfluenced by the structure's vibrations in order to increase their visibility. The lowest resonance frequency (about 2.1 Hz, clearly visible at all sensors along the deck) was observed on the transversal component (T). Hence, this resonance frequency is interpreted as the first translational mode of vibration of the bridge.

On the other hand, the lowest resonance frequency for both the vertical and longitudinal components is identified between 3.8 and 3.9 Hz (hereafter 3.85 Hz). These two frequencies might correspond to two distinct, but very close, transversal and longitudinal modes of vibration. However, considering that the bridge's deck is obviously bound at its longitudinal extremities, and thus its stiffness is expected to be larger along the longitudinal direction than along the
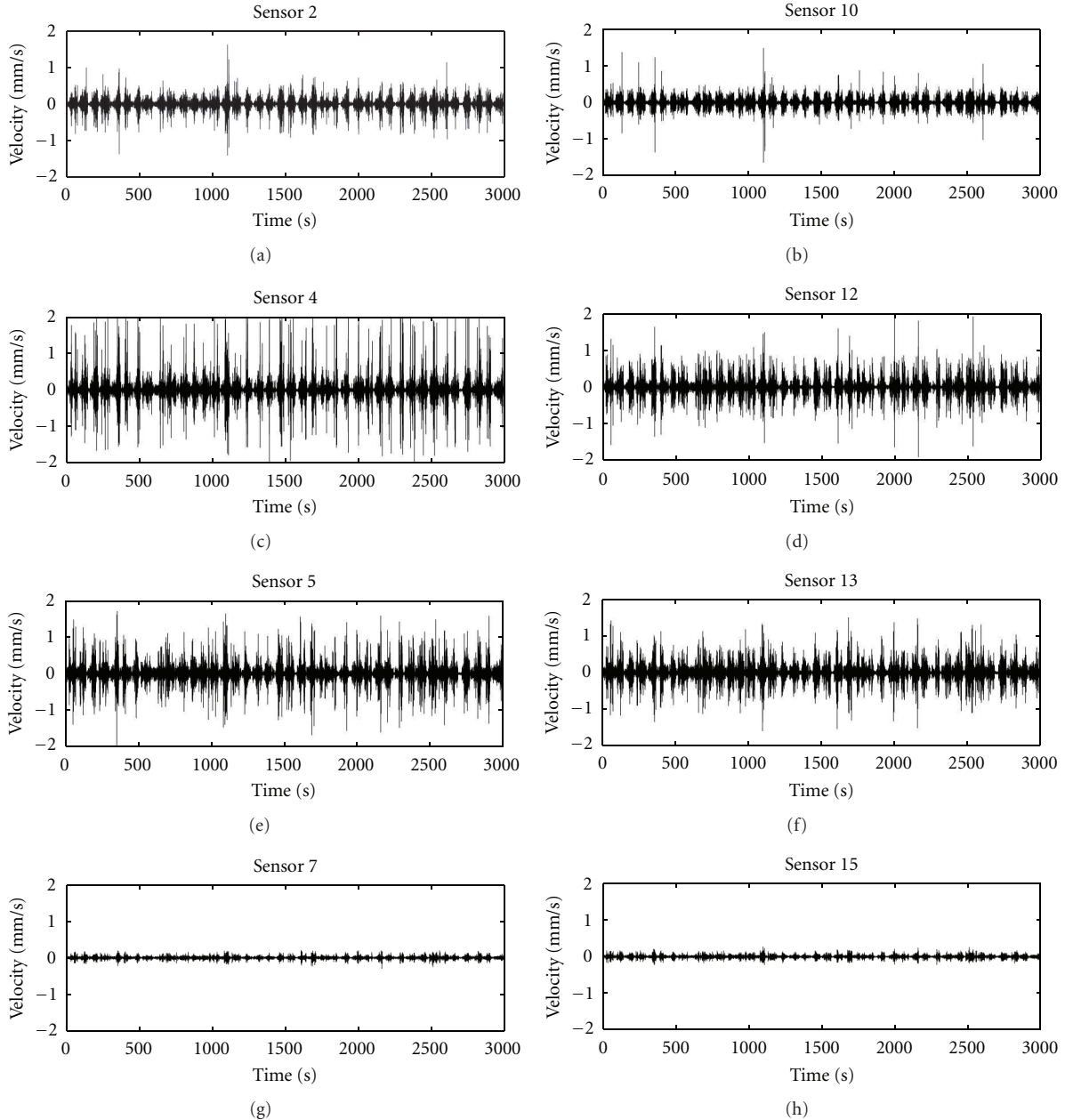
FIGURE 2: Recorded ambient vibrations (vertical component) at 8 sensors (see also Figure 1(c)) along the two sides of the bridge deck in the time period from 10:00 to 10:50 UTC. Note the large number of transient signals, which are due to the traffic crossing the bridge. Also note the variations in amplitude of the signals along the bridge deck.

vertical one, the first longitudinal mode of vibration should be at higher frequency than the vertical one. For this reason, and also considering the intrinsic uncertainty associated with spectral peak estimation, we believe that the first vertical mode of vibration is associated to a rocking motion (*V-L*), and thus the spectral peak along the longitudinal direction is only a component of the motion along the vertical one.

In order to better identify the higher resonance frequencies, it is instructive to plot the PSDs obtained at the different sensors along the bridge deck together in a plot with a linear *y*-axis, which makes the identification of peaks that are consistently present at all sensors easier (Figure 6(b)), while the

log-log plots shown in Figures 3, 4, and 5 allow for a better visualization of the finer structure of the spectra at individual sensors. Hence, Figure 6(b) allows the identification of the main frequencies of vibration of the structure. In summary, we identified a total of seven frequencies of vibration for the bridge (Table 1) at 2.1, 3.85, 4, 4.7, 6.4, 7.1, and 9.4 Hz. In particular, the frequencies 4 and 4.7 Hz correspond to the third and fourth translational modes on the transversal and vertical components, respectively. The frequency 6.4 Hz is identified on both the vertical and longitudinal components, thus the fifth mode is interpreted as rocking. Furthermore, the frequency 7.1 Hz is observed on all the components, but
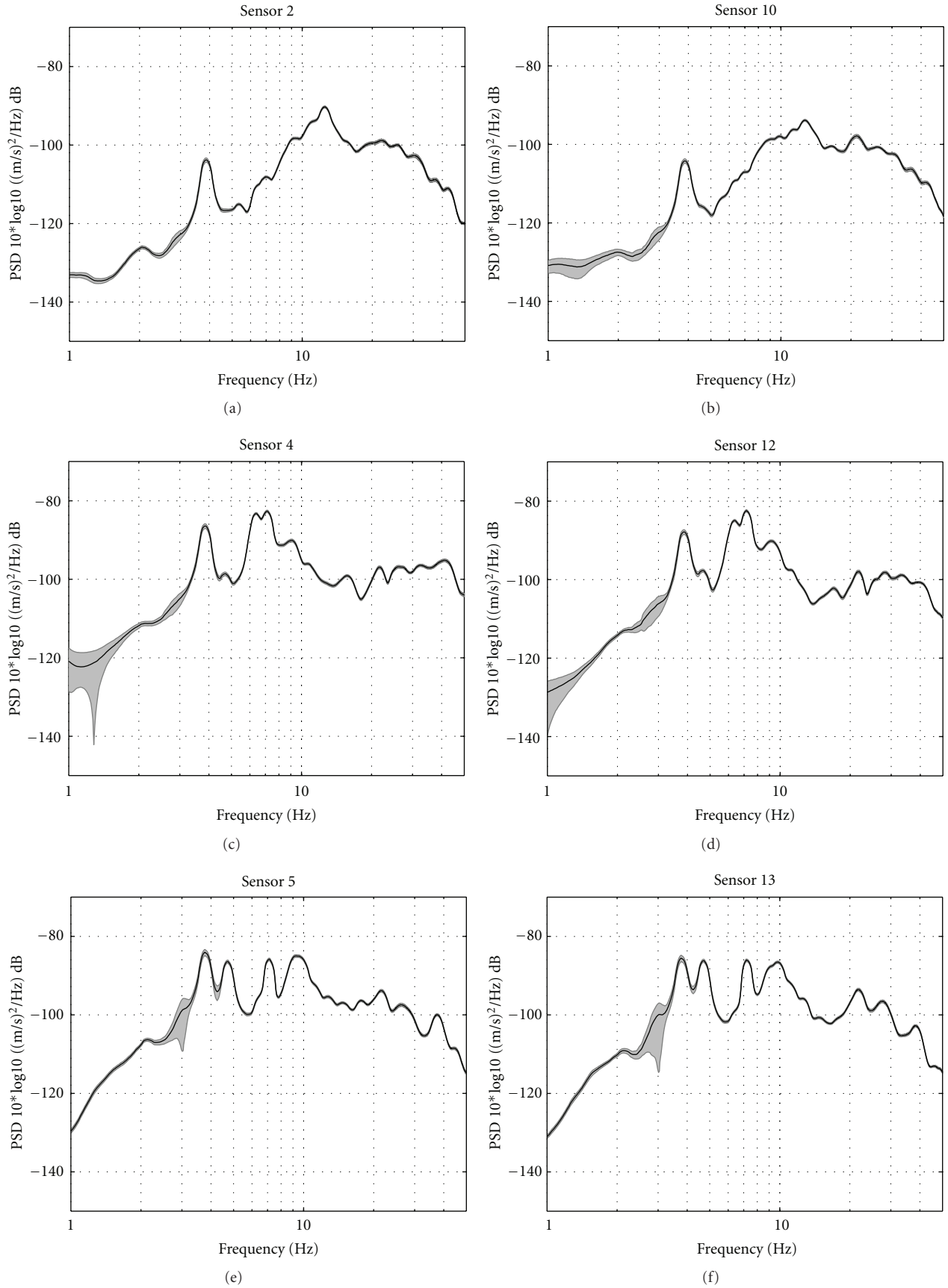
(a)

(b)

(c)

(d)

(e)
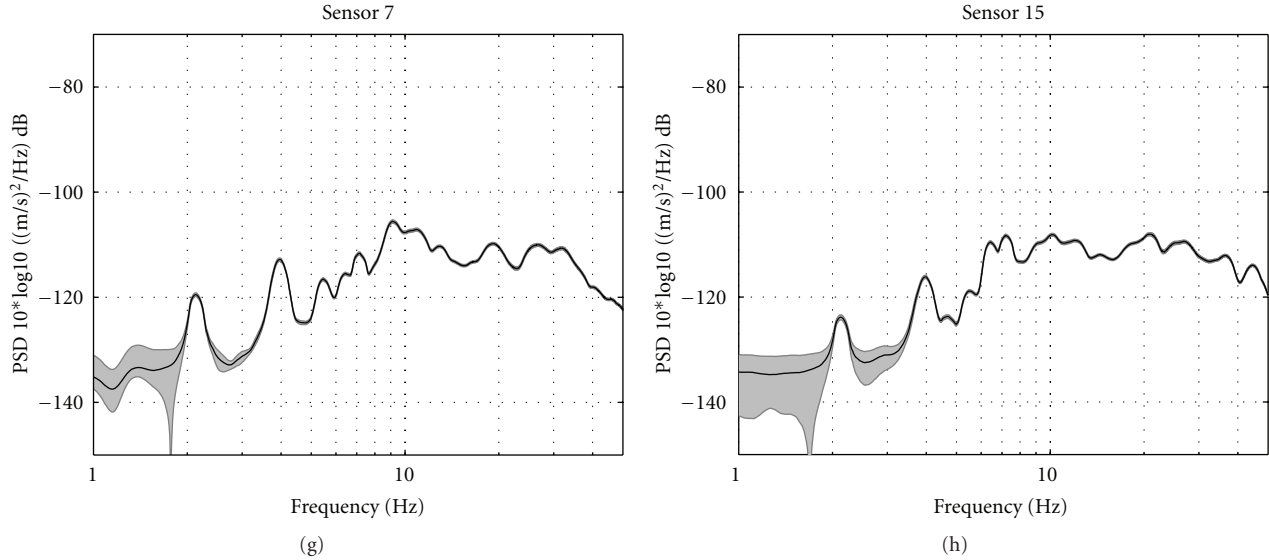
(f)

Figure 3: Continued.

(g)

(h)

FIGURE 3: Fourier power spectral density (PSD) (vertical component) calculated over the time span 10:00–15:00 UTC at the 8 sensors for which time series examples have been shown in Figure 3.

TABLE 1: Modal frequencies of vibration of the Adolphe Bridge for the three components of motion. The values assembled in this table are also indicated in Figure 6(b) as black dashed lines.

Mode I translat. (T–dir.) f (Hz)	Mode II rocking (V-L–dir.) f (Hz)	Mode III translat. (T–dir.) f (Hz)	Mode IV translat. (V–dir.) f (Hz)	Mode V rocking (V-L–dir.) f (Hz)	Mode VI translat. (V–dir.) f (Hz)	Mode VII translat. (T–dir.) f (Hz)
2.1	3.85	4	4.7	6.4	7.1	9.4

with the highest amplitude on the vertical one. Hence, we consider the sixth mode as mainly translational, but affected by a minor component of rotation and rocking. Finally, we noted that, for most of the sensors and components, but especially for the transversal one, the highest amplitude peaks in the PSDs are related to a higher frequency at about 9.4 Hz. We consider this to be the seventh translational mode. However, we are aware that this last frequency might be corrupted by the presence of near-field sources as cars drive along the bridge deck in close proximity to the sensor locations.

On the side of the Upper City, at sensors 7 and 15, a smaller peak also appears in the vertical component PSDs at a frequency of 2.1 Hz (Figure 3). Since this peak corresponds exactly to the fundamental frequency seen on the transversal component, a first-order interpretation could be that the appearance of this peak provides indications that not only translational, but also rotational modes play a role in the structural behavior, leading to a coupling between the different measured components. The same observation is also made on the longitudinal component, where the effect is even clearer than on the vertical at most of the sensors, except for the bridge center (Figure 5).

As the above analysis shows, one obvious advantage of a monitoring system composed of a large number of these low-cost WSUs is that not only changes in the spectral characteristics over time at one or a few points of the structure can be measured, but the structure can also be spatially densely sampled at a reasonable cost. This allows for a better understanding of the dynamic characteristics of different parts of the structure. On the Adolphe Bridge, we can see that there is a change in the PSD at frequencies higher than the fundamental one along the deck, reflecting the composition of the bridge, with the large span arches in the middle and smaller arches on each side of the central ones.

5. Modal Shapes of Vibration

In addition to the characteristics of the PSD estimates calculated along the bridge deck, which can serve as proxies for real-time monitoring purposes to detect changes in the bridge's response to input vibrations, another interesting point is how the different sensors along the bridge deck move with respect to each other or, in other words, how the bridge deforms at each mode of resonance.

To investigate this issue, we empirically calculated the modal shapes for the first four modal frequencies assembled in Table 1 of each component of motion following Meli et al. [14]. The normalized modal shapes obtained for different 249 one-minute time windows are plotted in Figure 7. Note that, for the distance scale, we used the location of sensors 2 and 10 as reference, that is, zero distance (Figure 7).
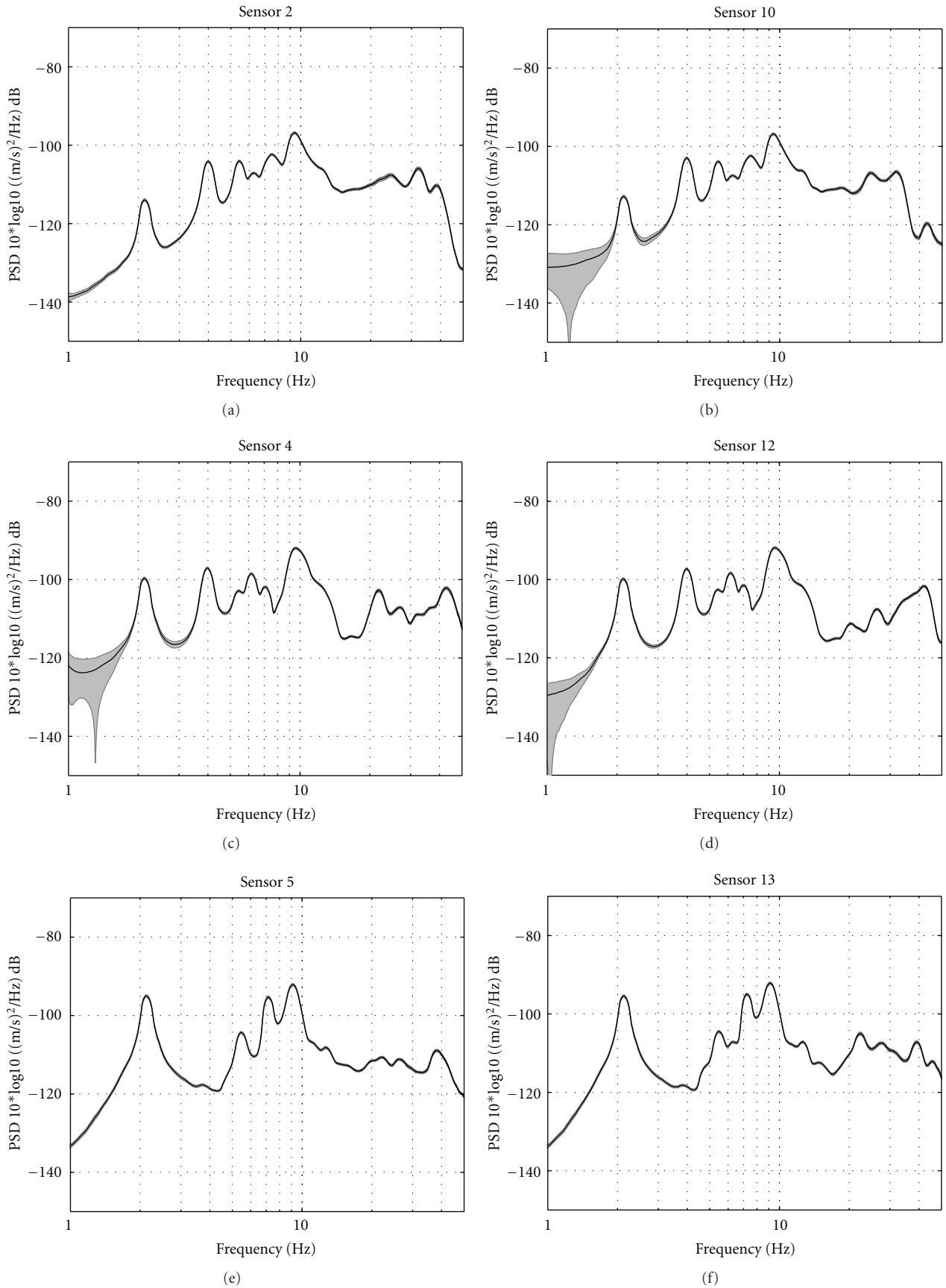
(a)

(b)

(c)

(d)

(e)

(f)
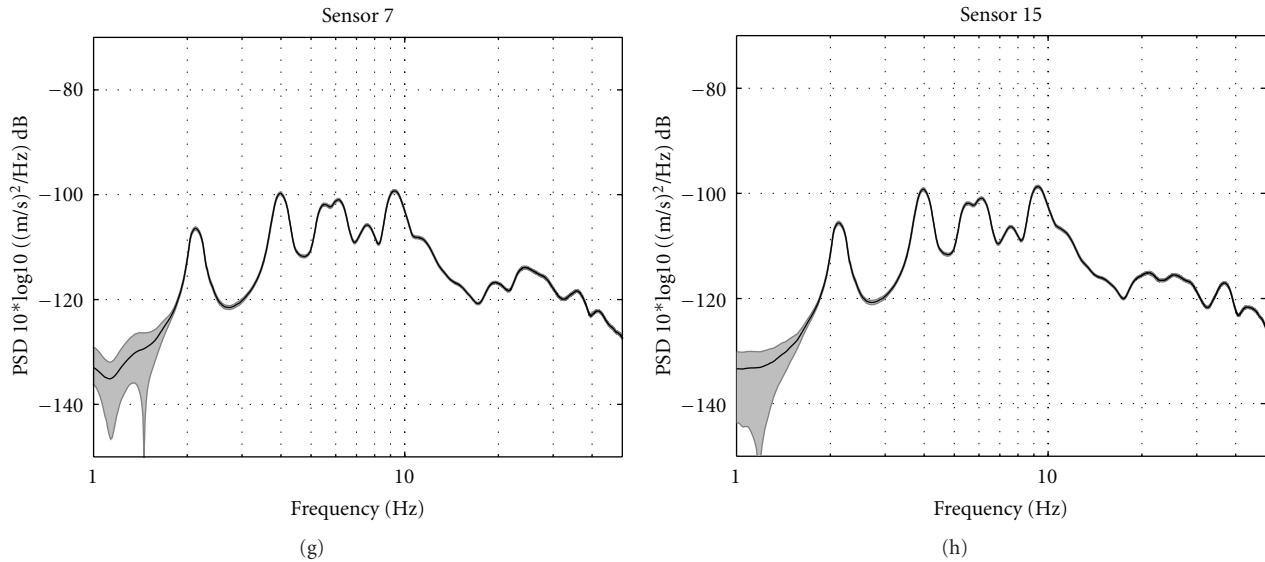
FIGURE 4: Continued.

(g)

(h)

Figure 4: Same as Figure 3, but for the transversal component.

Moreover, we did not consider sensors 1 and 9 in the calculation of the modal shape since these were located on the outermost pillars towards the railway station side.

Figure 7 shows an example of the obtained dominant modal shape families at four of the investigated modal frequencies (each line represents the modal shape calculated for a one-minute time window) derived for the transversal component on the left side of the deck. We performed this analysis for both sides of the bridge deck (i.e., sensors 2–8 and sensors 10–16) and combined the observations of the average modal shapes (i.e., the average of the dominant families) on both sides of the deck into surface plots for the transversal (Figure 8), vertical (Figure 9), and longitudinal (Figure 10) components.

The modal shapes for the transversal component at both sides of the bridge deck show consistent results (Figure 8). At the fundamental frequency of 2.1 Hz, the entire bridge deck is moving either to the left or to the right, with the largest amplitude in the center. This is comparable to the motion of a vibrating string expected at its fundamental frequency, indicating that the deck of the bridge behaves more or less as a single unit in terms of transverse motions. The same observation holds true for the next higher mode at 4.0 Hz, for which again the modal shape looks similar to what would be expected for the first overtone normal mode of a vibrating string. Yet for the next higher modal shape at a frequency of 7.2 Hz, a large amplitude is observed only for the sensor at the center of the arch. Finally, for the highest considered modal frequency of 9.4 Hz, the motion becomes rather complex. However, we should note that for these last two higher modes, the number of sensors and/or the geometry of the array selected might not guarantee a sufficient resolution for the reconstruction of the wavelengths associated with the modal shapes.

In the vertical component case (Figure 9), the determined modal shapes on the left and right side are consistent with one another and, at the fundamental frequency of 3.85 Hz, the central arches move in the opposite direction to the smaller arches on each side of them. As one may expect, the strongest motion is observed in the center of the bridge. The modal shape for the next higher mode at 4.7 Hz shows very similar characteristics, while the two highest modes (6.4 Hz and 7.1 Hz) show strongest motions in the side arches. Differently from the clear modal shapes pattern observed for the transversal direction, which agrees with the schema expected for the global motion of the bridge, the similarity of modal shapes along the vertical one was unexpected and raised some interpretational issues. Indeed, this modal shapes similarity may be related either to the lack of adequate resolution or to the presence of local motion of some of the bridge's elements (e.g., the deck, the slab, etc.).

Finally, for the longitudinal component (representing compression/dilatation of the deck, Figure 10), we observe a similar behavior as for the transverse component for the first modal frequency (3.85 Hz), which as we discussed is related to a rocking motion. In particular, we observe that all the sensors show common phase, and the motion is larger at the center of the deck. However, starting from the second mode, we note that the two opposite sides of the deck seem to show different behavior. Similarly to what we observed for the vertical component, we cannot exclude neither the hypothesis that we recorded a global motion of the bridge with an inadequate spatial resolution, nor that the observed modal shapes are related to local motion of some of the bridge's elements. These observations would clearly deserve further investigation with an even denser network, which would allow to sample more finely the bridge and thus have greater confidence in the modal shapes for the higher modes, as well as contributing to discussions with structural engineers in terms of the potential consequences of this type of observation.
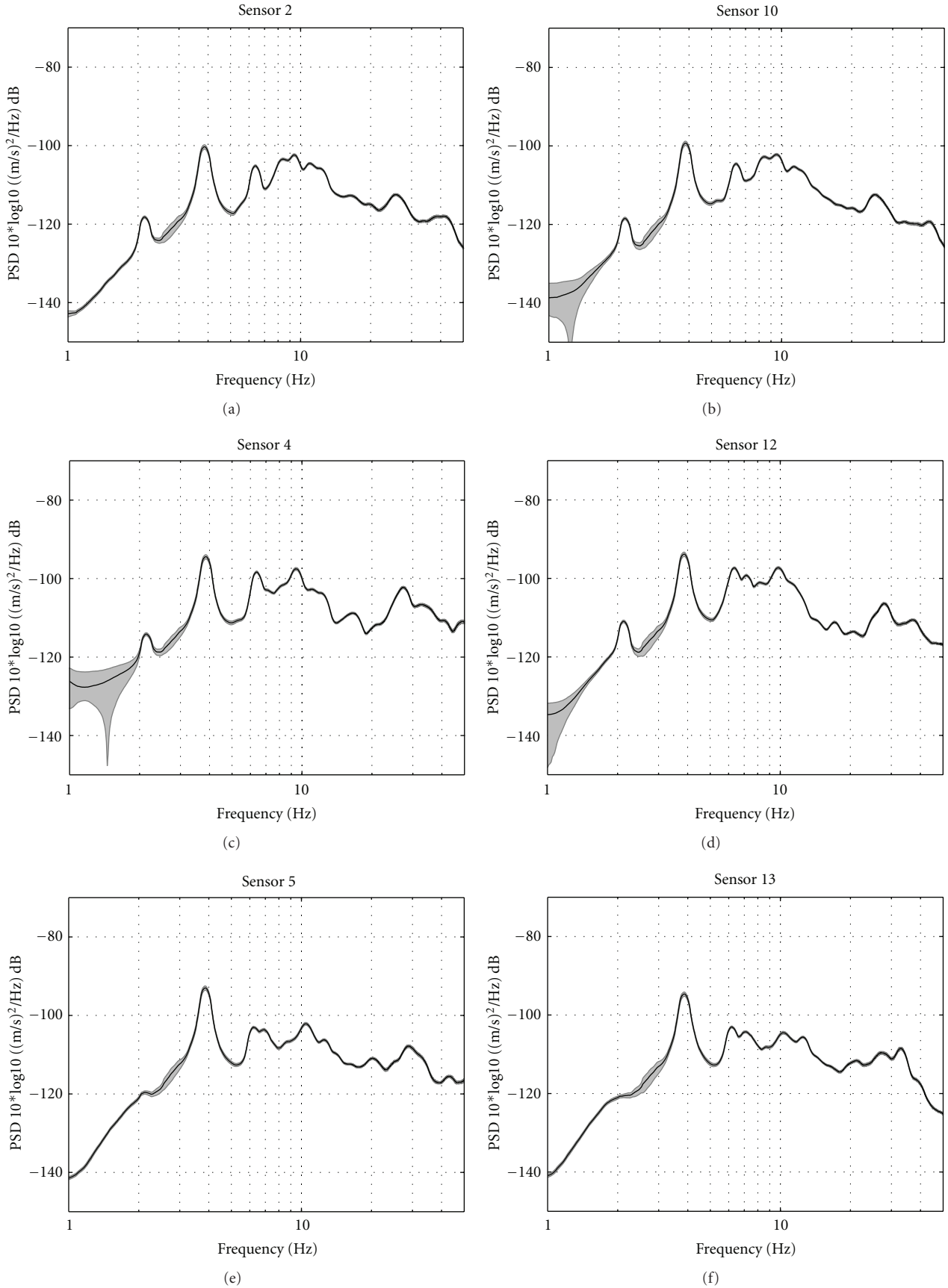
(a)

(b)

(c)

(d)

(e)

(f)
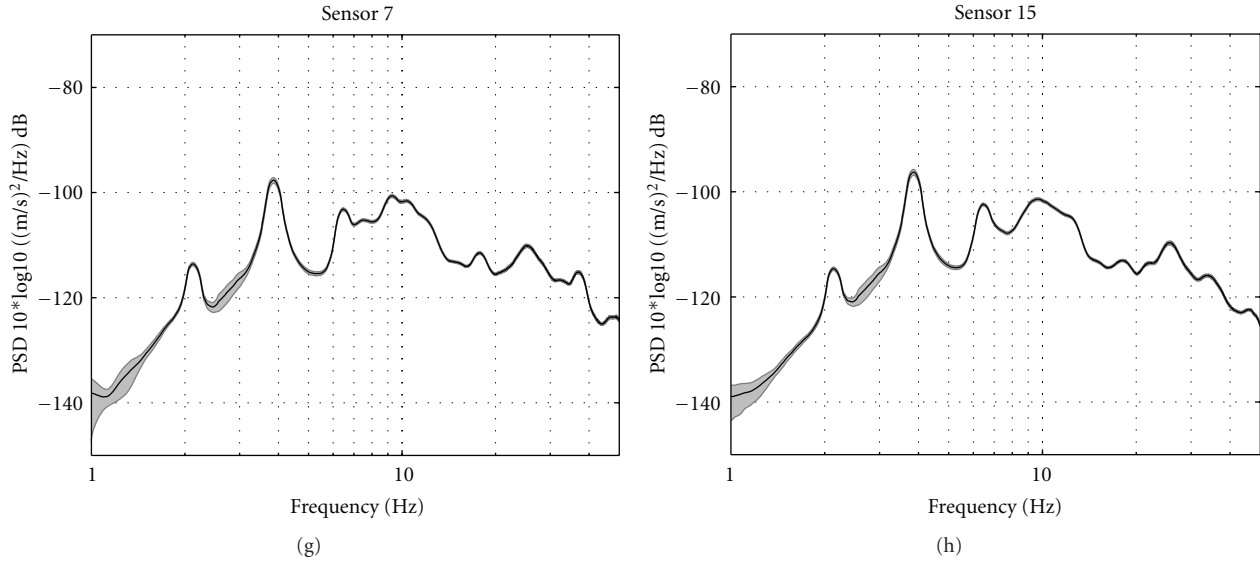
Figure 5: Continued.

(g)

(h)

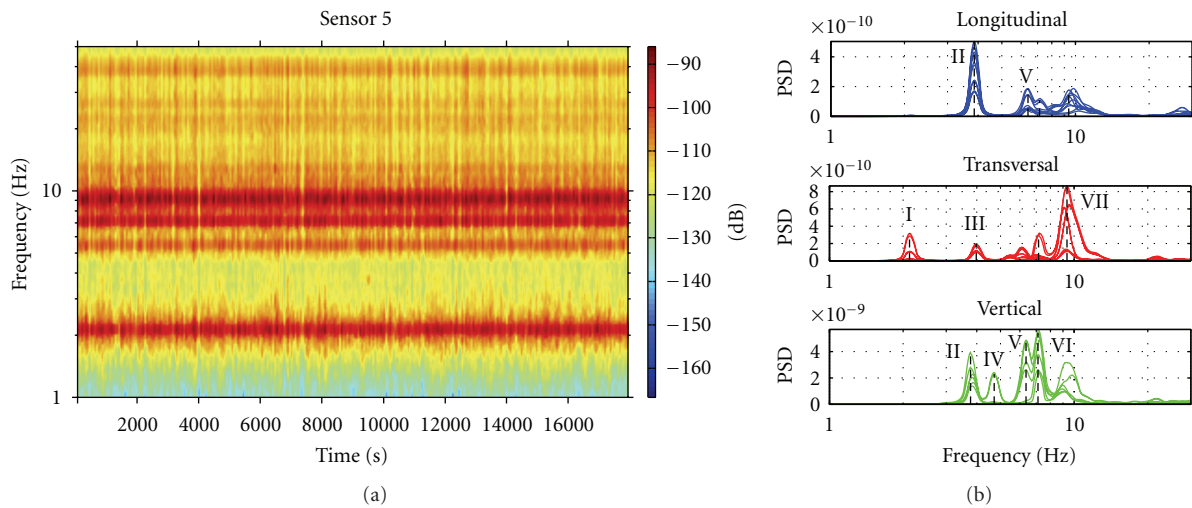FIGURE 5: Same as Figures 3 and 4, but for the longitudinal component.

(a)

(b)

FIGURE 6: (a) Example for the spectrograms (sensor 5, transversal component) over the 5-hour time window (10:00–15:00 UTC). Please compare with the PSD estimate at sensor 5 shown in Figure 4. (b) PSD estimates of sensors on both sides along the bridge deck plotted together for each component on a log-linear scale. Black dashed lines: frequencies of the vibration modes considered for deriving the modal shapes of the bridge. The modes are annotated by their roman number, as given in Table 1.

6. Damping Estimates Using the NonPaDAn Approach

Finally, we attempted to derive an estimate of the damping at the fundamental frequency using the NonPaDAn (nonparametric damping analysis) method introduced by Mucciarelli and Gallipoli [15] for use with ambient vibration recordings, which was recently used for the extensive dynamic characterization of Italian and European buildings [16].

In summary, this approach works in the time domain and consists of the following steps: first, after standard processing procedures, the velocity time series are integrated to displacement time series. Then, all positive values of the time series that represent local maxima are selected, and their amplitudes (A_i for the ith maximum) and times of occurrence (t_i for the ith maximum) are stored in a matrix. If for the ith maximum the condition $A_i > A_{i+1}$ holds, an estimate of pseudofrequency ν and damping γ is calculated as (equations 2.2 and 2.3 in [15])

$$\nu = \frac{1}{(t_{i+1} - t_i)}, \qquad \gamma = \left(\frac{1}{2\pi}\right) \cdot \left(\frac{A_i}{A_{i+1}}\right). \qquad (1)$$

From these estimates, a histogram can then be build considering piecewise pseudo-frequency and damping values. Furthermore, NonPaDAn also provides damping estimates by means of empirical cumulative distributions (CDFs), from which the median and the 25th and 75th percentile can be extracted. Mucciarelli and Gallipoli [15] showed that
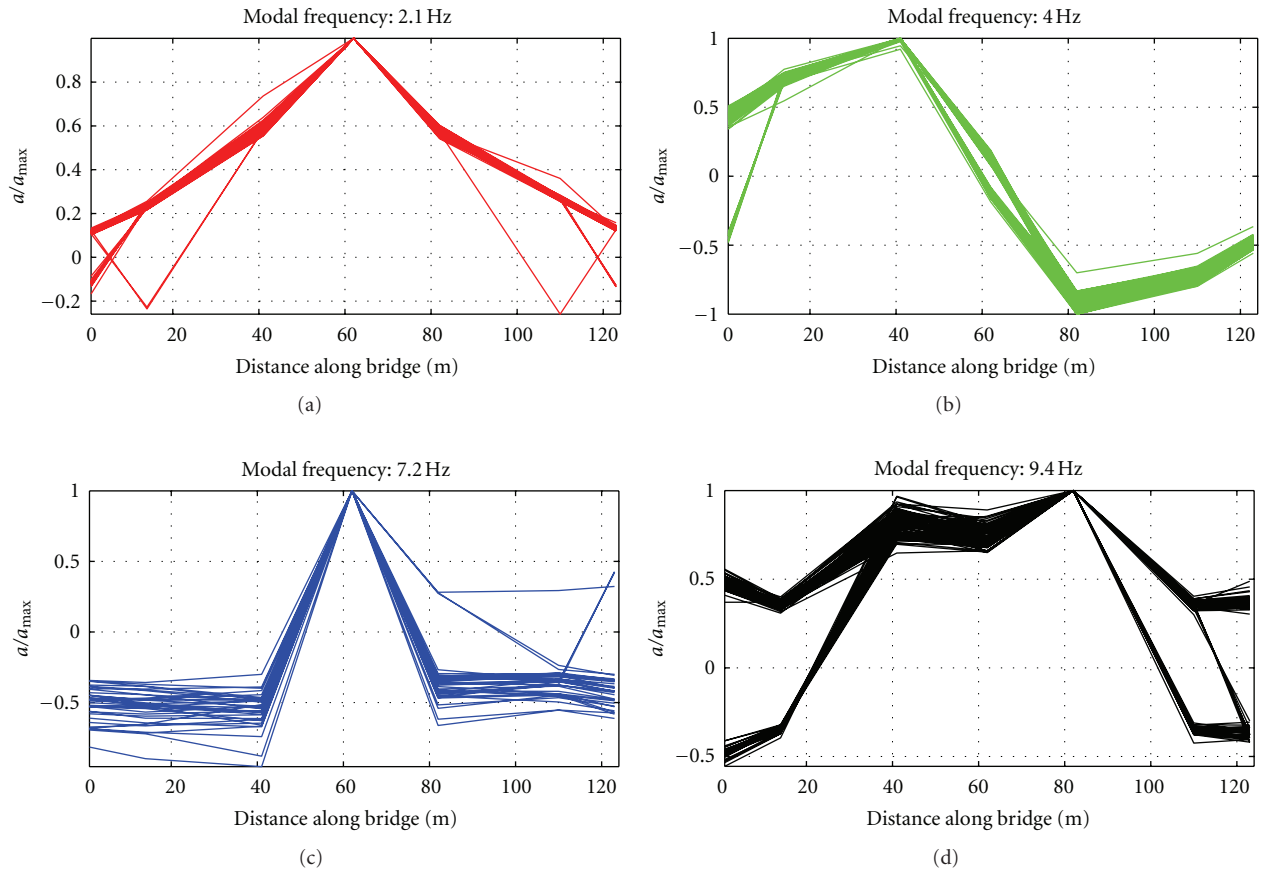
(a)

(b)

(c)

(d)

FIGURE 7: Example of the derivation of the modal shapes (transverse component, left side of deck) of vibration for the fundamental mode of resonance (upper left, red) and the three higher modal frequencies presented in Figure 6(b) and listed in Table 1. For each modal frequency, each individual line represents the modal shape derived from a one-minute time window. More details on the derivation are given in the text.

the approach is able to capture the fundamental frequency and damping values using ambient vibration recordings (even with rather short-duration recordings of only several minutes) made atop a building, while the higher modes are rarely visible.

Concerning the estimation of the damping in the Adolphe bridge case, we focused on the sensors 5 and 13, which are located in the middle of the central arches. As a first test, we verified the stability of the NonPaDAn procedure by considering different lengths of recording period. Figure 11 shows the CDFs of damping estimated for the fundamental frequency 3.85 on the longitudinal component using periods of 30, 60, and 120 minutes, respectively. It is worth noting that the damping estimates are very stable even when only few tens of minutes are considered. Therefore, we adopted 30 minutes as standard recording length for this purpose.

As observed by Mucciarelli and Gallipoli [15], we also noted that, in the case of different resonance frequencies with similar amplitudes, the CDF estimated when considering the entire histogram can be a mixed, corrupted version of the CDFs for different resonance frequencies. In our experiment, we observed that, in most cases, the frequency 9.4 Hz is the dominant signal. As a result, the CDFs

estimates also turned out to be strongly influenced by this frequency. If, for instance, a higher-frequency mode strongly dominates the PSD estimates (e.g., transversal component of sensors 4 and 12, with about 15 dB higher amplitude of the 9.4 Hz overtone as compared with the fundamental mode at 2.1 Hz, see Figure 4), NonPaDAn captures only the overtone vibrations, however, generally without a clear maximum in the histogram and rather strong smearing over a range of damping values. For this reason, we slightly modified the NonPaDAn code and constrained the CDF analysis on a narrow frequency band (i.e., ± 1 Hz) centered around a selected resonance frequency. In practical terms, we simply restrict the calculation of the CDF to the part of the histogram within ± 1 Hz of the resonance frequency of interest, that is, we reduce the sample analyzed in the CDF calculation to those data where the estimated pseudo-frequency $v(1)$ was within ± 1 Hz of the resonance frequency of interest.

Figures 12 and 13 show the histograms and the CDFs of the damping for the transversal, longitudinal, and vertical components observed at sensors 5 and 13, respectively. As can be seen from the histograms (upper panels), both the fundamental as well as the higher modes are visible in the NonPaDAn histograms. As a general rule, we observe that

Modal frequency: 2.1 Hz

(a)

Modal frequency: 4 Hz

(b)

Modal frequency: 7.2 Hz
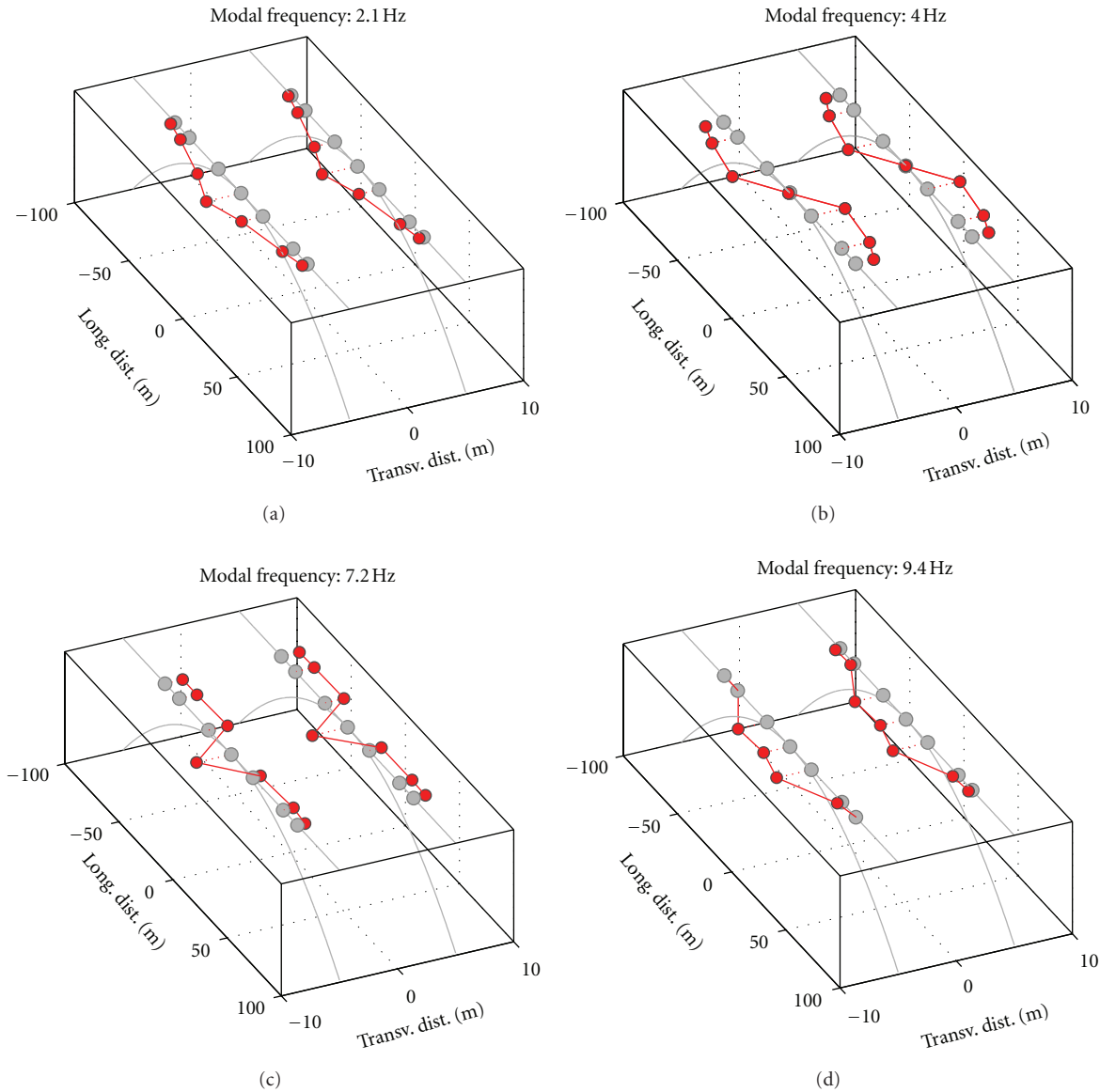
(c)

Modal frequency: 9.4 Hz

(d)

FIGURE 8: Modal shapes (transversal component) illustrating the motion of the entire deck in the transversal direction. Note that the relative amplitude of displacement in the transverse direction is exaggerated.

the histograms reflect the observed PSD shapes at each sensor (i.e., if a given mode of vibration dominates in the PSD estimate, it will also be dominant in the NonPaDAn histograms).

It is interesting to note that the two sensors provide damping estimates in excellent agreement with each other and that the horizontal components of motion show lower damping than the vertical one. The CDFs follow reasonably well a log-normal distribution, with similar shape on both sides of the bridge and median damping values ranging around 2–4% for the fundamental modes on the horizontal components and around 9% on the vertical one. While for the horizontal components the distributions are narrow (25th and 75th percentiles are shown as gray dots in Figures 12(b) and 13(b)) and thus the damping is rather well constrained, for the vertical component the interval between

the 25th and 75th percentile covers a broader damping range (i.e., approximately 5 to 13%).

Thus, we conclude that in, the case of a strongly excited fundamental mode vibration, it is possible to derive an estimate of the bridge's damping for this vibration. However, the analysis is much more complicated for the cases of dominating higher modes, and careful visual inspection of the results at each individual sensor and component is required to avoid erroneous conclusions. Such complications, when compared with the experience of Mucciarelli and Gallipoli [15] who applied such an approach to buildings, may be related to the fact that the Adolphe Bridge represents a very different setting compared to the analysis of recordings obtained from atop a building. Contrasting with our experience on the Adolphe Bridge, in the cases of buildings shown by Mucciarelli and Gallipoli [15], NonPaDAn generally only
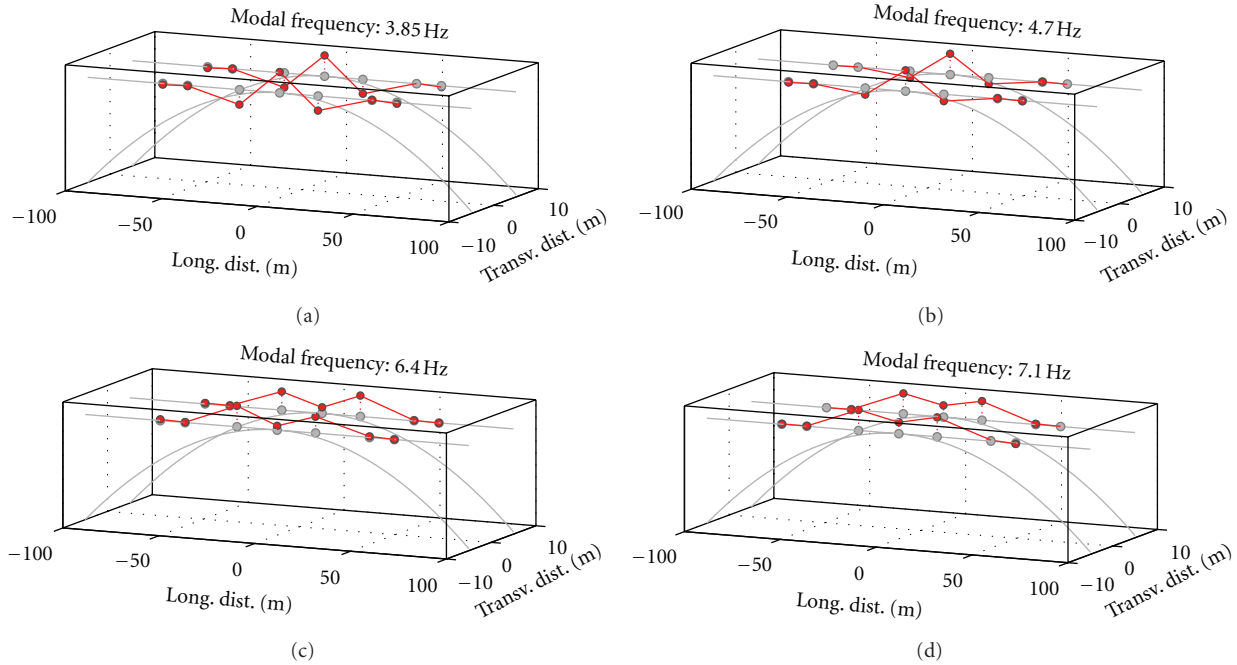
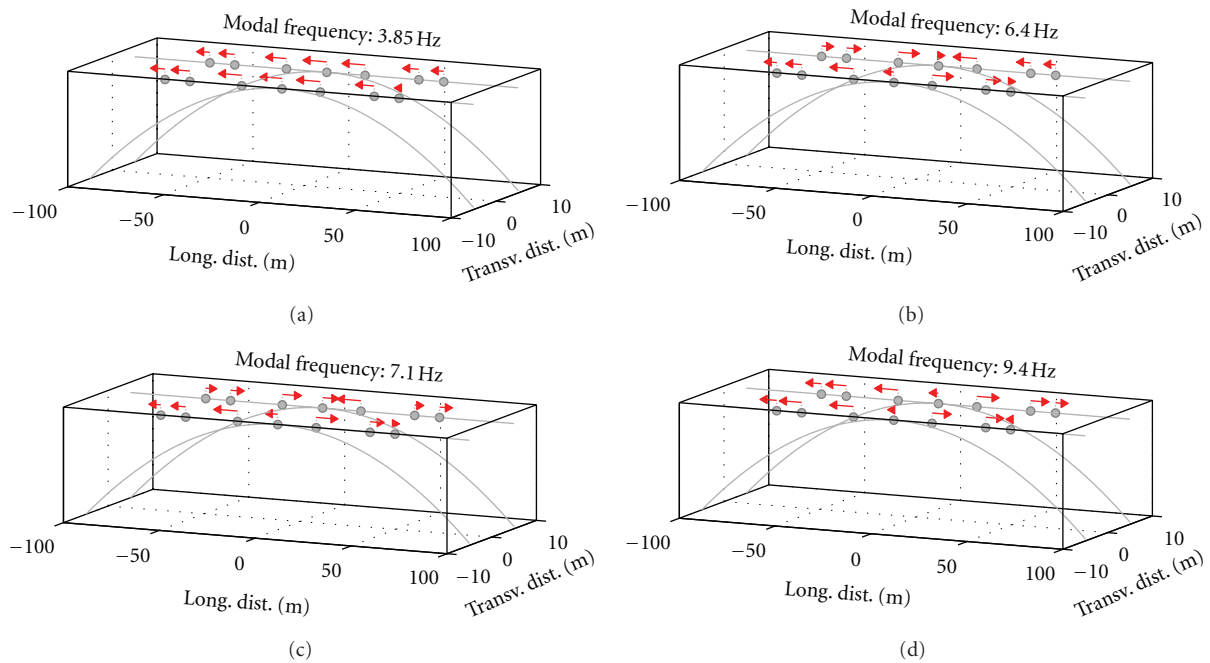Figure 9: Same as **Figure 8**, but for the vertical component.

Figure 10: Same as Figures 8 and 9, but for the longitudinal component, that is, compression/dilatation of the bridge deck. Note that the relative direction of motion and amplitude of displacement in the longitudinal direction are represented through the arrow direction and length, respectively.

captures the fundamental mode of vibration. In contrast to a building where the seismic source exciting the structure is always consistently applied at the base (except, of course, for the case of strong wind excitations), the sources are in our case heterogeneously distributed along the structure of interest, both in space and time. Furthermore, the transient signals caused by cars crossing the bridge can follow each other at very short time intervals and be superposed to create a complicated signal resulting from the highly complex distribution of moving sources, making the evaluation of damping difficult and most likely the primary reason for the smearing effects seen in the histograms.
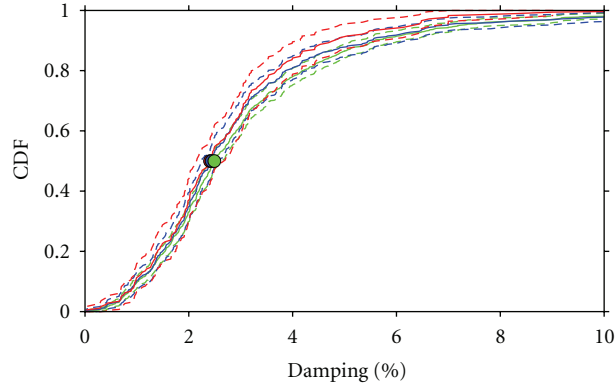
FIGURE 11: Comparison of CDFs of damping derived for the fundamental mode on the longitudinal component considering different recording lengths, that is, 30′ (red), 60′ (blue), and 120′ (green).
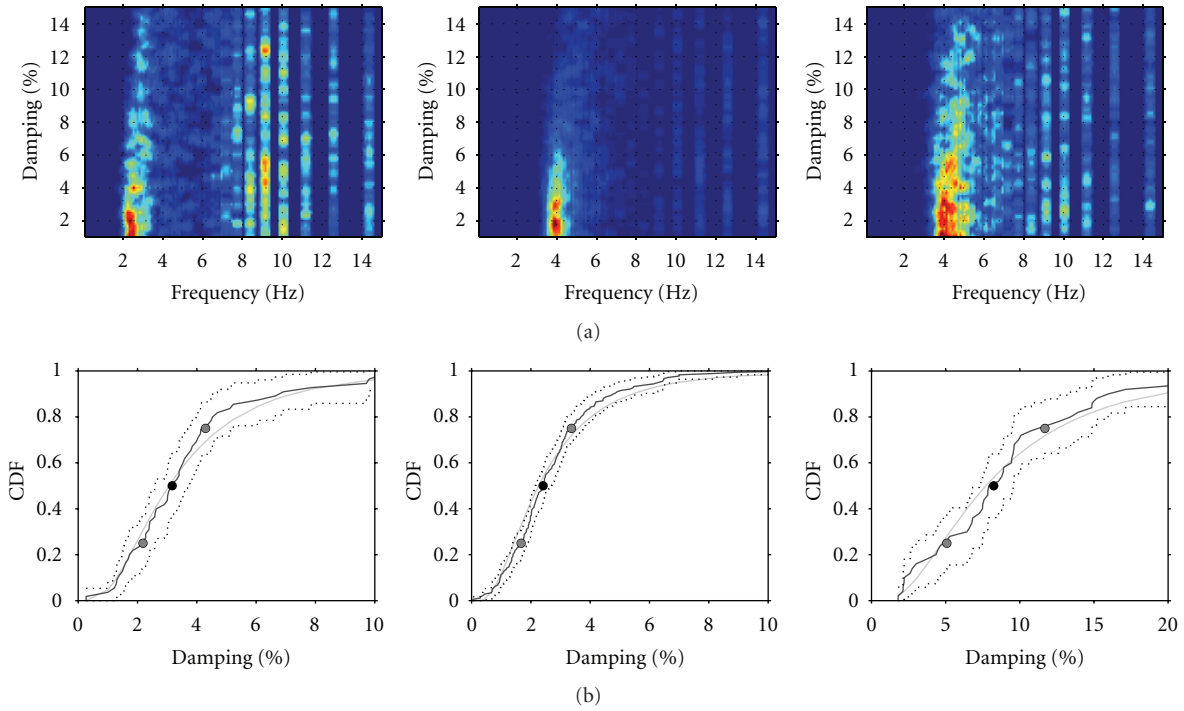

(a)

(b)

FIGURE 12: (a) Histograms (binned frequency and damping) derived using the NonPaDAn approach for sensor 5 for the transversal (left panel), longitudinal (central panel), and vertical (right panel) components. (b) Same order as (a), but showing the CDFs of the damping estimated for the fundamental frequency. More details are provided in the text.

7. Conclusions

We have presented the results of an experiment for the structural monitoring of a historical masonry arch bridge, the Adolphe Bridge in Luxembourg City, using a set of 18 low-cost wireless sensing units. From the five hours of ambient vibration recordings analyzed, we were able to clearly identify the fundamental frequencies of resonance for the three components of bridge motion (vertical, transversal, and longitudinal) as well as several higher modes for each component. While on the vertical and longitudinal components, the fundamental frequency of resonance is around 4 Hz (which, remarkably, is in good agreement with

a forced vibration experiment performed in 1933 on the original bridge deck [10]), the fundamental frequency of the transversal component is at around 2 Hz. Furthermore, the high stability of PSD estimates and the spectrograms show that, if necessary, a rapid assessment of the bridge's dynamic behavior is possible using such campaign-type experiments. It should be noted that, while a wealth of information can be gained from such a temporary experiment, as shown in this paper, a significantly more detailed understanding of the entire bridge (and not only of the bridge deck) could be obtained by installing a permanent monitoring system, including within the arch structure, the latter being difficult to access to at regular intervals for campaign-type
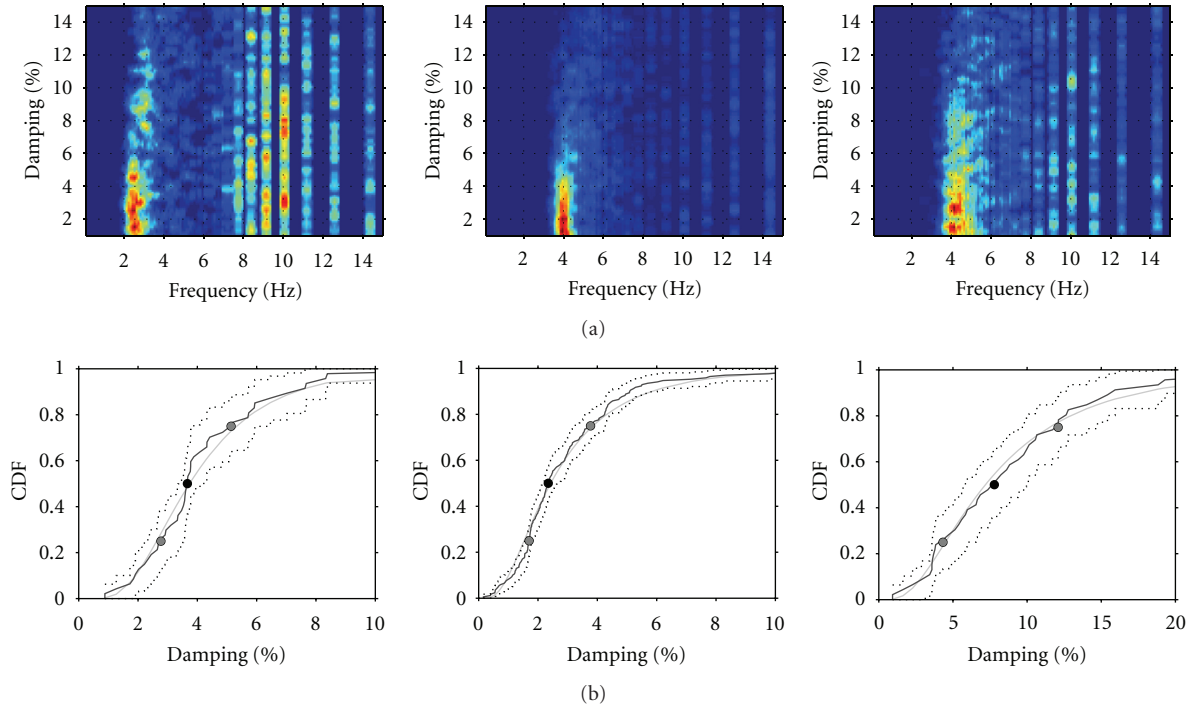
(a)

(b)

FIGURE 13: Same as Figure 12, but for sensor 13 (opposite of sensor 5, i.e., in the middle of the central arch on the right side of the bridge deck).

deployments. Such a monitoring system could provide real-time information on the dynamic characteristics of the bridge and their potential modifications that may be of concern, for instance, during heavy storm events.

Furthermore, we were able to empirically extract the modal shapes of the bridge's vibrations, which provide very interesting insights into the dynamic behavior of the structure. These modal shapes show that, with respect to the transversal component, the bridge deck displays a global motion characterized by a deformation pattern similar to the modal shapes of a simple string. The modal shapes observed for the vertical and longitudinal directions are more complicated, especially for the higher modes, and might be related to the local motion of some of the bridge's elements. This result surely deserves further investigation, considering that it may be related to differences in the structural response of the two arches composing the bridge. Furthermore, the modal shapes obtained in this experiment could be refined deploying an even denser spatial sampling on each side of the bridge (i.e., more sensors, which were however unfortunately not available at the time of the experiment). Nevertheless, our results clearly indicate the great potential that ambient vibration measurements using these low-cost wireless sensors hold for the monitoring of such structures.

We adopted the NonPaDAn procedure in order to estimate the damping at the most significant location along the bridge (i.e., in the center of the largest-span arches). We noted that, in the case of bridge monitoring by ambient vibrations, the analysis can be strongly complicated by the presence of dominating higher modes. This complication,

when compared to the experience of Mucciarelli and Gallipoli [15] who applied the approach to buildings, may be related to the fact that the Adolphe Bridge represents a very different setting compared to the analysis of recordings obtained on top of buildings. Nevertheless, the damping estimations obtained for the sensors located at the middle of the central arches on opposite sides of the deck are consistent with each other and are very stable. We observed rather low damping values for the horizontal components (i.e., 2–4%) and a damping of about 9% for the vertical one.

The results of this experiment demonstrate the great potential for using such a system of wireless sensing units as a tool for permanent monitoring of the Adolphe Bridge following the upcoming renovation works. Upon reopening of the bridge to traffic, the system could be used to detect potential structural degradations over the years to come on a continuous basis. Moreover, once the tram system is operating again in Luxembourg in several years time, it also has the potential of monitoring the excitation of the bridge related to the tram traffic, allowing for the timely recognition of potential problems and, consequently, the rapid response to them.

Boxberger and Hippolyte Jacob for their assistance during the experiment and to Kevin Fleming for kindly correcting their English. The constructive comments of an anonymous referee are highly appreciated.

References

[1] M. Picozzi, R. Ditommaso, S. Parolai et al., "Real time monitoring of structures in task force missions: the example of the Mw = 6.3 Central Italy Earthquake, April 6, 2009," *Natural Hazards*, vol. 52, no. 2, pp. 253–256, 2010.

[2] J. P. Lynch, *Decentralization of wireless monitoring and control technologies for smart civil structures*, Ph.D. thesis, Department of Civil and Environmental Engineering, Stanford University, Stanford, Calif, USA, 2002.

[3] C. U. Grosse, F. Finck, J. H. Kurz, and H. W. Reinhardt, "Monitoring techniques based on wireless AE sensors for large structures in civil engineering," in *Proceedings of the 26th European Conference on AE testing*, vol. 90, pp. 843–856, Berlin, Germany, 2004.

[4] M. Krüger, C. U. Große, and P. J. Marrón, "Wireless structural health monitoring using MEMS," *Key Engineering Materials*, vol. 293-294, pp. 625–634, 2005.

[5] R. Ditommaso, S. Parolai, M. Mucciarelli, S. Eggert, M. Sobiesiak, and J. Zschau, "Monitoring the response and the back-radiated energy of a building subjected to ambient vibration and impulsive action: the Falkenhof Tower (Potsdam, Germany)," *Bulletin of Earthquake Engineering*, vol. 8, no. 3, pp. 705–722, 2010.

[6] G. A. Prieto, J. F. Lawrence, A. I. Chung, and M. D. Kohler, "Impulse response of civil structures from ambient noise analysis," *Bulletin of the Seismological Society of America*, vol. 100, no. 5 A, pp. 2322–2328, 2010.

[7] M. Picozzi, C. Milkereit, C. Zulfikar et al., "Wireless technologies for the monitoring of strategic civil infrastructures: an ambient vibration test on the Fatih Sultan Mehmet Suspension Bridge in Istanbul, Turkey," *Bulletin of Earthquake Engineering*, vol. 8, no. 3, pp. 671–691, 2010.

[8] A. Wirion and R. Heinerscheid, "Le pont Adolphe à Luxembourg: historique de l'ouvrage: considérations sur les modes d'exécution adoptés par P. Séjourné," *Revue Technique Luxembourgeoise*, vol. 4, pp. 228–247, 1953 (French).

[9] Luxembourgish Government Press Release, Le Pont Adolphe à Luxembourg, Service Information et Presse, 2005, http://www.gouvernement.lu/salle_presse/actualite/2005/08/04wiseler_pont_adolphe/Dossier-presse-nouveau.pdf, (in French).

[10] M. Ros, "Bericht über die Schwingungsversuche vom 21. Oktober 1933 auf der Pont Adolphe über die Petrusse in Luxemburg," Report to the Département des Travaux Publics du Grand-Duché de Luxembourg, Zurich, Switzerland, 1934.

[11] M. Picozzi, C. Milkereit, S. Parolai et al., "GFZ wireless seismic array (GFZ-WISE), a wireless mesh network of seismic sensors: new perspectives for seismic noise array investigations and site monitoring," *Sensors*, vol. 10, no. 4, pp. 3280–3304, 2010.

[12] K. Fleming, M. Picozzi, C. Milkereit et al., "The self-organizing seismic early warning information network (SOSEWIN)," *Seismological Research Letters*, vol. 80, no. 5, pp. 755–771, 2009.

[13] D. E. McNamara and R. P. Buland, "Ambiente noise levels in the continental United States," *Bulletin of the Seismological Society of America*, vol. 94, no. 4, pp. 1517–1527, 2004.

[14] R. Meli, E. Faccioli, D. Murià-Vila, R. Quaas, and R. Paolucci, "A study of site effects and seismic response of an instrumented building in Mexico city," *Journal of Earthquake Engineering*, vol. 2, no. 1, pp. 89–111, 1998.

[15] M. Mucciarelli and M. R. Gallipoli, "Non-parametric analysis of a single seismometric recording to obtain building dynamic parameters," *Annals of Geophysics*, vol. 50, no. 2, pp. 259–266, 2007.

[16] M. R. Gallipoli, M. Mucciarelli, and M. Vona, "Empirical estimate of fundamental frequencies and damping for Italian buildings," *Earthquake Engineering and Structural Dynamics*, vol. 38, no. 8, pp. 973–988, 2009.